UDC 669.2, 669.046.584
https://doi.org/10.17073/0021-3438-2025-2-5-18

Research article
Научная статья

Characterization of an atypical intermediate layer formed in Vanyukov furnaces during smelting of charges with a high content of technogenic materials

L.V. Krupnov[1,3], **R.A. Pakhomov**[2], **A.V. Kaverzin**[3], **Ya.I. Kosov**[2], **P.V. Malakhov**[1]

[1] Polar Division of **PJSC "MMC "Norilsk Nickel"**
2 Gvardeyskaya sq., Norilsk 663302, Russia

[2] **LLC Gipronickel Institute**
11 Grazhdansky Prosp., Saint-Petersburg 195220, Russia

[3] **N.M. Fedorovsky Polar State University**
7 50-Let Oktyabrya Str., Norilsk 663310, Russia

✉ Leonid V. Krupnov (KrupnovLV@nornik.ru)

Abstract: The growing need for recycling, along with the depletion of high-grade ore concentrates, has led to the inclusion of previously accumulated technogenic materials — such as metallurgical slags, sludge from settling ponds of recirculating water systems, and similar waste— into the charge of primary smelting units. The share of such feedstock in the furnace charge now reaches approximately 25 %, which has resulted in serious technological disruptions to the stable operation of primary autogenous smelting units. In Vanyukov furnaces, this is manifested by the appearance – alongside the typical smelting products (matte and slag) – of a new atypical phase, the so-called intermediate layer. The formation of this layer leads to adverse effects, including the obstruction of flow paths from the furnace hearth to the slag and matte siphons, ultimately causing a complete shutdown of the unit. A sample of this abnormal product, collected from an industrial furnace during a period of process instability, was analyzed using differential scanning calorimetry (DSC), thermogravimetric analysis (TGA), and differential thermal analysis (DTA). These methods allowed the determination of temperature ranges corresponding to phase transformations of the components comprising the intermediate layer. The results obtained can be used to define optimal parameters for stable smelting operation and to develop technical solutions that prevent conditions favorable for the formation of refractory accretions.

Key words: charge, technogenic feedstock, low-energy-value feedstock, liquid-bath smelting furnace, Vanyukov furnace, matte, slag, smelting products, oxysulfide phase, energy-dispersive *X*-ray microanalysis (EDS), differential thermal analysis (DTA).

Acknowledgments: The authors express their gratitude to the staff of the Norilsk Nickel R&D Center at the Institute of Non-Ferrous Metals, Siberian Federal University, who participated in the study: S.A. Silyanova, B.M. Lobastova, N.V. Nelyubina, A.S. Samoilo.

For citation: Krupnov L.V., Pakhomov R.A., Kaverzin A.V., Kosov Ya.I., Malakhov P.V. Characterization of an atypical intermediate layer formed in Vanyukov furnaces during smelting of charges with a high content of technogenic materials. *Izvestiya. Non-Ferrous Metallurgy*. 2025;31(2):5–18. https://doi.org/10.17073/0021-3438-2025-2-5-18

Изучение свойств атипичного продукта – «промежуточного слоя» печей Ванюкова, при переработке шихты с высоким содержанием техногенных продуктов

Л.В. Крупнов[1,3], **Р.А. Пахомов**[2], **А.В. Каверзин**[3], **Я.И. Косов**[2], **П.В. Малахов**[1]

[1] **Заполярный филиал ПАО «ГМК «Норильский никель»**
663302, Россия, Красноярский кр., г. Норильск, пл. Гвардейская, 2

[2] **ООО «Институт Гипроникель»**
195220, Россия, г. Санкт-Петербург, Гражданский пр-т, 11

[3] **Заполярный университет им. Н.М. Федоровского**
663310, Россия, Красноярский кр., г. Норильск, ул. 50 лет Октября, 7

✉ Леонид Владимирович Крупнов (KrupnovLV@nornik.ru)

Аннотация: Современные требования, определяющие необходимость рециклинга, а также снижение объемов качественных рудных концентратов привели к вовлечению в переработку на головных плавильных агрегатах ранее накопленного техногенного сырья – металлургических шлаков, илов прудов-отстойников систем оборотного водоснабжения и т.п. Доля такого сырья в загрузке плавильных агрегатов достигает уже ~25 %, что обусловило серьезные технологические сбои в устойчивом ведении процесса на головных автогенных плавильных агрегатах. Для печей Ванюкова это появление наряду с типичными продуктами плавки (штейна и шлака) нового атипичного продукта – так называемого промежуточного слоя, образование которого приводит к негативным последствиям, которые выражаются в запечатывании перетоков из горна печи в шлаковый и штейновый сифоны с последующей полной остановкой агрегата. Изучение такого аномального продукта, отобранного на промышленном агрегате в период отклонения от устойчивого ведения технологического процесса, методами дифференциально-сканирующей калориметрии, термогравиметрического и дифференциального термического анализа позволило определить температурные интервалы фазовых преобразований компонентов, входящих в состав промежуточного слоя. Полученные результаты помогут определить желаемые параметры устойчивого ведения процесса плавки и предложить технические решения, препятствующие неблагоприятным условиям настылеобразования.

Ключевые слова: шихта, техногенные продукты, низкоэнергетическое сырье, печь плавки в жидкой ванне, печь Ванюкова, штейн, шлак, продукты плавки, оксисульфидная фаза, рентгеноспектральный микроанализ (РСМА), дифференциальный термический анализ (ДТА).

Благодарности: Авторы благодарят сотрудников R&D Центра «Норникель» Института цветных металлов Сибирского федерального университета, принявших участие в работе: С.А. Сильянова, Б.М. Лобастова, Н.В. Нелюбина, А.С. Самойло.

Для цитирования: Крупнов Л.В., Пахомов Р.А., Каверзин А.В., Косов Я.И., Малахов П.В. Изучение свойств атипичного продукта – «промежуточного слоя» печей Ванюкова, при переработке шихты с высоким содержанием техногенных продуктов. *Известия вузов. Цветная металлургия*. 2025;31(2):5–18. https://doi.org/10.17073/0021-3438-2025-2-5-18

Introduction

At the Polar Division of PJSC “MMC Norilsk Nickel” (PD NN), copper pyrometallurgical operations involve processing of copper sulfide feedstock to produce copper anodes, which are then transferred to the electrorefining stage for the production of cathode copper. One of the feed materials used in the process is technogenic feedstock. Its use is necessitated by the depletion of high-quality ores and the implementation of environmental programs [1]. The production technology includes several sequentially arranged pyrometallurgical units, the primary of which is the Vanyukov furnace, a bath smelting unit. This is one of the modern and high-capacity pyrometallurgical units used to process copper sulfide materials. Global analogues of the Vanyukov furnace include bottom-blown smelting furnaces, Isasmelt (top-submerged lance) reactors, Mitsubishi process furnaces with multiple non-submerged tuyeres, flash smelting furnaces, and others [2—5].

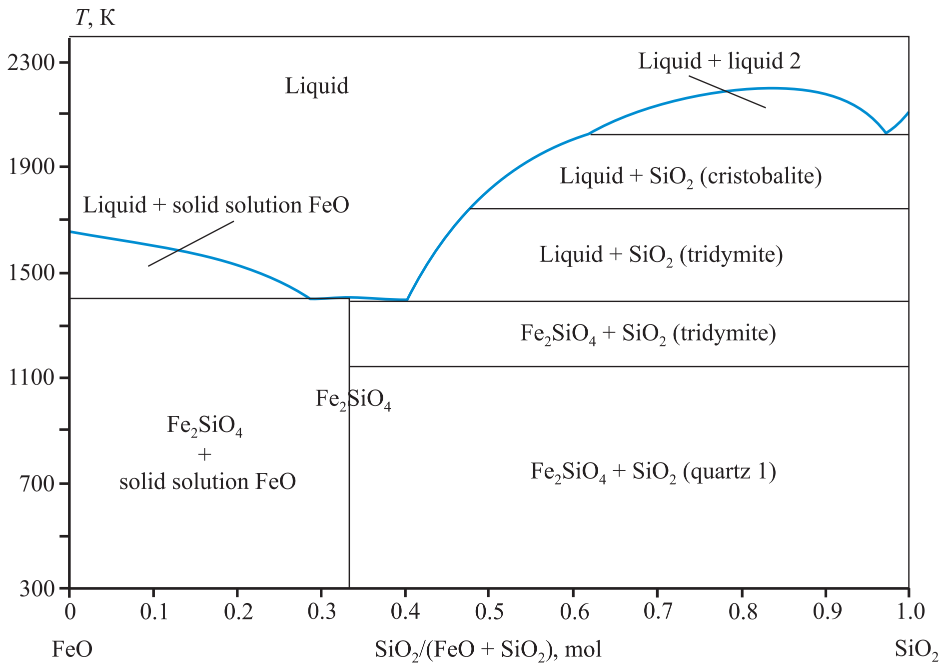

Fig. 1. Binary phase diagram of $FeO-SiO_2$ system

Рис. 1. Диаграмма состояния двойной системы $FeO-SiO_2$

In copper production at PD NN, silica-rich fluxes are used for slag formation. International industrial practice widely employs ferrosilicate slags in the processing of copper and copper-nickel sulfide feedstocks. Examples include the Olympic Dam smelter (Australia), Zhong Tiao Shan's Houma smelter (China), and Konkola Copper Mines (Zambia), among others [6—8]. The use of silica (SiO_2) as a fluxing agent significantly facilitates the oxidative blowing of sulfide feedstock by forming slags with relatively low melting points. The binary $FeO—SiO_2$ phase diagram is shown in Fig. 1.

However, variations in feed composition under constant oxidizing potential, disruption of process parameters, increased oxidant supply, natural gas shortages (used to compensate heat losses), and other factors may lead to the formation of high-melting compounds in the furnace atmosphere of pyrometallurgical units. These compounds are represented by spinel-type phases of variable composition containing non-ferrous metals [9; 10].

Since 2019, significant process disruptions have been observed in the operation of the Vanyukov furnace at the Copper Plant of PD NN due to considerable changes in the composition of the processed feedstock [11; 12]. One of the key issues has been impaired melt flow caused by a reduction in the cross-sectional area of the tapping channel. The narrowing of the flow path was attributed to the appearance of a new, atypical product in the smelting output — a so-called intermediate layer. This material forms a separate oxide phase with sulfide inclusions and occupies an interfacial position between the slag and matte phases [13]. The composition of this layer was initially unclear, necessitating further investigation into its origin and formation conditions.

Similar issues have been encountered in the operation of the most widespread technology for processing copper and nickel sulfide concentrates — flash smelting [14—18]. As the intermediate layer became saturated with magnetite, it led to the formation of a solid phase, which eventually settled on the hearth and slag zone of the furnace. To mitigate the risk of accretion formation, a set of technological and engineering measures was implemented, involving modifications to both the equipment and the process parameters. For instance, at the Kalgoorlie Nickel Smelter operated by WMC (Australia), lime was added to the feed mix to lower the slag melting point and improve its fluidity, the smelting temperature was raised to 1360 °C, and smelting and converting operations were integrated within a single unit by installing six electrodes in the settling zone [19—22].

The objective of this study was to determine the mechanism and formation conditions of the intermediate heterogeneous layer during smelting in Vanyukov furnaces at the Copper Plant of PD NN, and to develop recommendations for ensuring stable operation at this production stage.

Research methodology

The study was based on a sample of the intermediate layer collected in October 2023. The formation of this sample during that period was associated with a deterioration in the composition of the processed charge. The sample represented an oxysulfide product (Fig. 2), in which oxide and sulfide regions of the intermediate layer were distinguishe. In this study, the two phases wee examined separately.

The atypical smelting product was studied using thermogravimetric analysis (TGA), differential thermal analysis (DTA), differential scanning calorimetry (DSC), *X*-ray diffraction analysis (XRD) [23—25], scanning electron microscopy (SEM), and energy-dispersive *X*-ray spectroscopy (EDS). It is worth noting that this combination of methods is widely applied in the study of technogenic material recycling and non-ferrous slag processing [26—32].

XRD analysis was performed using a Shimadzu XRD7000 diffractometer (Japan); thermal analysis (DTA and TGA) was carried out using Setsys Evolution-1750 (Setaram) and NETZSCH STA 409 PC/PG (Germany) thermal analyzers; SEM and EDS were performed using a Tescan 5130MM scanning electron microscope equipped with an Oxford Instruments INCA Energy microanalysis system and a YAG crystal as a backscattered electron detector. Analytical chemistry methods were applied using iCAP 6500 Duo SSEA and iCAP 7600 Radial atomic emission spectrometers (Thermo Scientific, USA). Thermodynamic modeling was conducted using the FactSage software package (version 6.4.1, 2012).

The content of major elements in the sulfide and oxide parts of the intermediate layer is presented in Table 1.

Results of sulfide phase analysis

The elemental composition (see Table 1), *X*-ray diffraction analysis (XRD, Fig. 3), scanning electron microscopy (SEM), and energy-dispersive *X*-ray spectroscopy (EDS, Fig. 4) of the sulfide phase indicate that

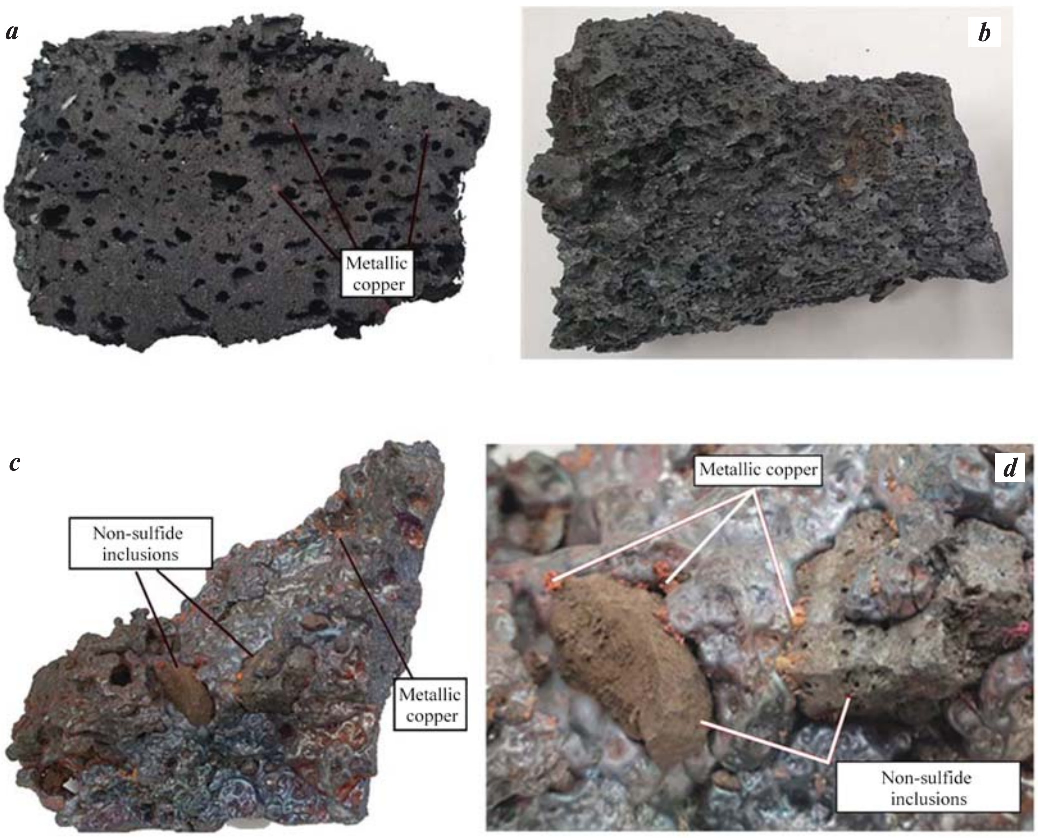

Fig. 2. General view of the atypical smelting product – intermediate layer: oxide phase (***a***, ***b***) and sulfide phase (***c***, ***d***)

Рис. 2. Общий вид атипичного продукта плавки – промежуточного слоя: оксидной (***a***, ***b***) и сульфидной (***c***, ***d***) фаз

Table 1. **Elemental composition of the analyzed samples**

Таблица 1. Элементный состав исследуемых проб

Component	Content of major elements, wt. %												
	Fe	Ni	Si	Cu	Al	Ti	Mg	Zn	Na	Ca	Co	K	S
Oxide phase	31.77	8.87	7.96	3.59	2.38	2.34	2.29	0.79	0.75	0.62	0.54	0.21	0.18
Sulfide phase	0.32	5.19	0.49	59.27	0.29	0.13	0.15	–	0.2	–	–	–	33.74

it is close in composition to typical copper matte. The results of the bulk chemical analysis (Table 1) are consistent with the phase composition data obtained by XRD, SEM, and EDS. The main components of the sulfide portion of the intermediate layer are copper (Cu, 59.27 wt. %) and sulfur (S, 33.74 wt. %), along with a notable nickel (Ni) content of 5.19 wt. %. The contents of other elements do not exceed 0.5 wt. %. According to the XRD data, the dominant phase in the sulfide portion is chalcocite (Cu_2S) (Fig. 3). The SEM and EDS analyses reveal additional mineral phases, including metallic solid solutions based on Cu—Ni alloys (Fig. 4, *c*), skeletal crystals of bunsenite (NiO) (Fig. 4, *c*, *d*), as well as less common olivine-group minerals such as liebenbergite (Ni_2SiO_4) (Fig. 4, *d*) and heazlewoodite (Ni_3S_2) (Fig. 4, *b*).

The conducted study demonstrated that the sulfide portion of the intermediate layer consists of distinct sulfide and metallic phases embedded in a structure of high-melting-point oxide material.

TGA and DTA of the sulfide phase were carried out under an argon atmosphere at a heating rate of 30 °C/min up to a maximum temperature of 1100 °C. The resulting thermogram is shown in Fig. 5. The data indicate that mass loss begins gradually at approximately 400 °C and accelerates above 700 °C. This behavior may

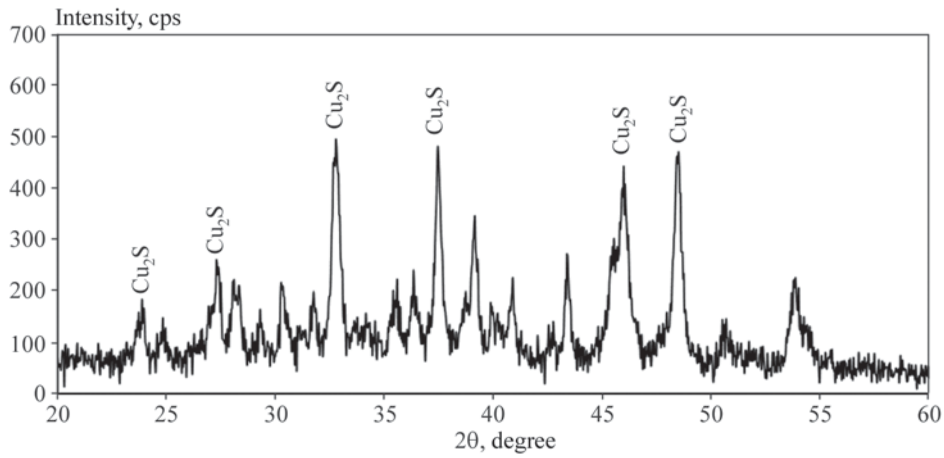

Fig. 3. *X*-ray diffraction pattern of the sulfide portion of the intermediate layer

Рис. 3. Рентгенограмма сульфидной части (промежуточного слоя)

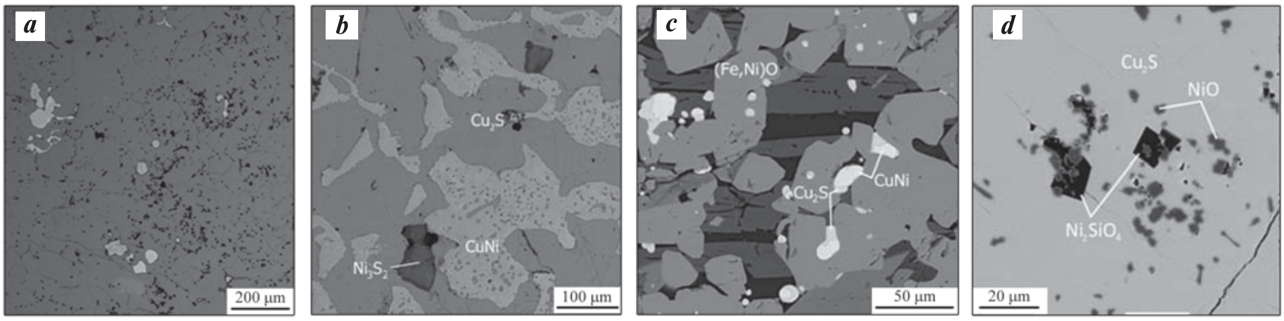

Fig. 4. General view of the sulfide sample (***a***) and phase distribution (***b***–***d***) in the analyzed material

Рис. 4. Общий вид проб сульфидной части (***a***) и распределение фаз (***b***–***d***) в исследуемой пробе

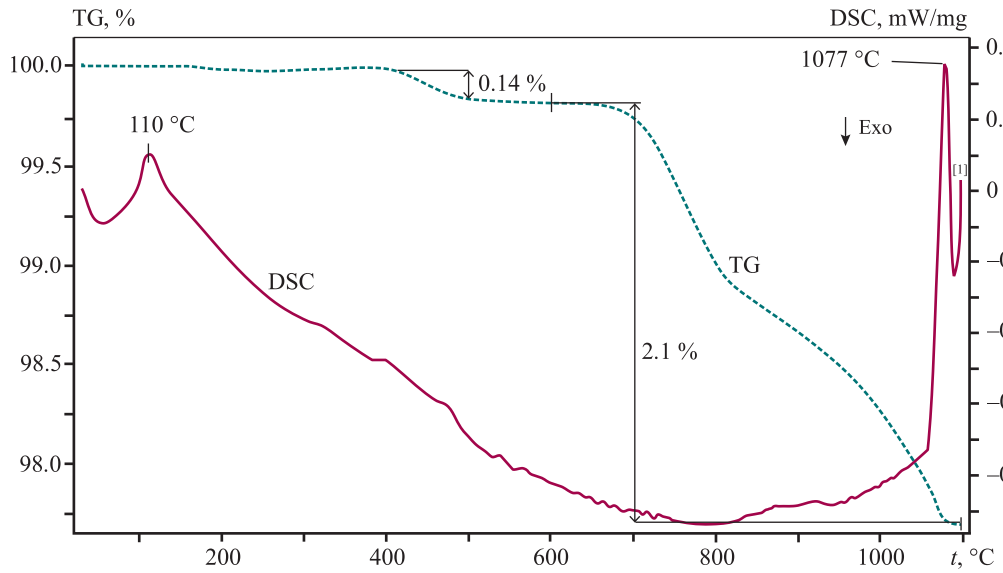

Fig. 5. Thermogravimetric and differential scanning calorimetry (DSC) results for the sulfide portion of the intermediate layer

Рис. 5. Общий вид результатов ТГА и ДСК для сульфидной части промежуточного слоя

be associated with the release of sulfur from Cu_2S, either due to the β-to-δ phase transition of Cu_2S or through δ-Cu_2S dissociation accompanied by sulfur volatilization. The apparent endothermic effect observed at 110 °C may be attributed to the relatively large sample mass (101 mg), which caused significant baseline drift in the DSC signal. Endothermic events recorded at 1077 °C and 1100 °C correspond to phase transition and subsequent melting of Cu_2S (which, according to phase diagrams, occurs at 1067 °C and 1105 °C, respectively) [33].

Results of oxide phase analysis

The main elements in the oxide portion of the intermediate layer are Fe (31.77 wt. %) and O (37.35 wt. %). Nickel and silicon are present in subordinate amounts (~8 wt. %), while copper, aluminum, titanium, and magnesium are found in the range of 2—3 wt. %. The contents of other elements do not exceed 1 wt. %.

X-ray diffraction analysis (XRD, Fig. 6) of the oxide phase showed that the sample contains spinel-type phases (magnetite), delafossite, cuprite, the tetragonal modification of SiO_2, and forsterite. SEM and EDS analyses further revealed that the oxide phase is compositionally and structurally homogeneous. The bulk of the sample is represented by oxide phases of variable composition, with a total volume fraction of approximately 80—95 %. In addition to the above phases, the sample also contains: a complex silicate component in the amount of 10—15 vol. % (pyroxene, clinopyroxene); dispersed metallic copper particles with minor iron content, up to 160 μm in size, with a total volume fraction not exceeding 0.1 %; and metallic copper with inclusions of cuprous oxide (Cu_2O).

Microstructural images of the oxide phase are presented in Fig. 7.

Additional analysis of the oxide portion was carried out using TGA and DTA, as was done for the sulfide part. The sample was tested under both inert (Ar) and oxidizing (O_2) atmospheres. The heating rate in both cases was 15 °C/min to a maximum of 1450 °C, and the cooling rate was 30 °C/min. The thermogram of the oxide portion of the intermediate layer is shown in Fig. 8. The analysis showed that in an inert atmosphere, the sample mass remained unchanged. However, two endothermic effects were observed, starting at approximately 1057 °C (with a peak at 1110 °C) and 1355 °C. The exact peak of the second effect could not be determined due to the temperature limit of the equipment (1450 °C). The first effect is attributed to the melting of metallic copper present in the intermediate layer. The second effect is tentatively associated with the onset of magnetite melting; however, complete melting of this primary phase was not observed at these temperatures. This is consistent with literature data [34, 35], according to which the melting point of magnetite exceeds 1590 °C.

In an oxidizing atmosphere (Fig. 8, *c*, *d*), two exothermic effects accompanied by mass gain were observed. These may be associated with partial oxidation of metallic or monovalent copper (Cu_2O, $CuFeO_2$) followed by decomposition at temperatures above 1000 °C to divalent copper oxide.

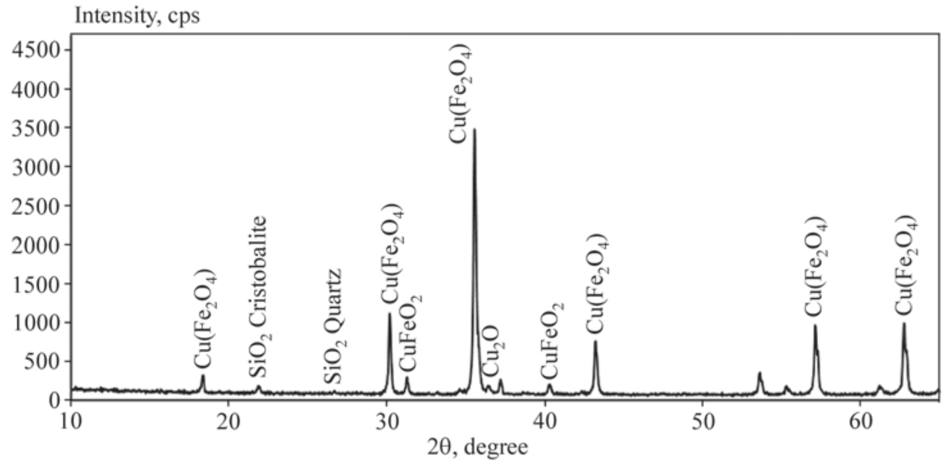

Fig. 6. *X*-ray diffraction pattern of the oxide portion of the intermediate layer

Рис. 6. Рентгенограмма оксидной части промежуточного слоя

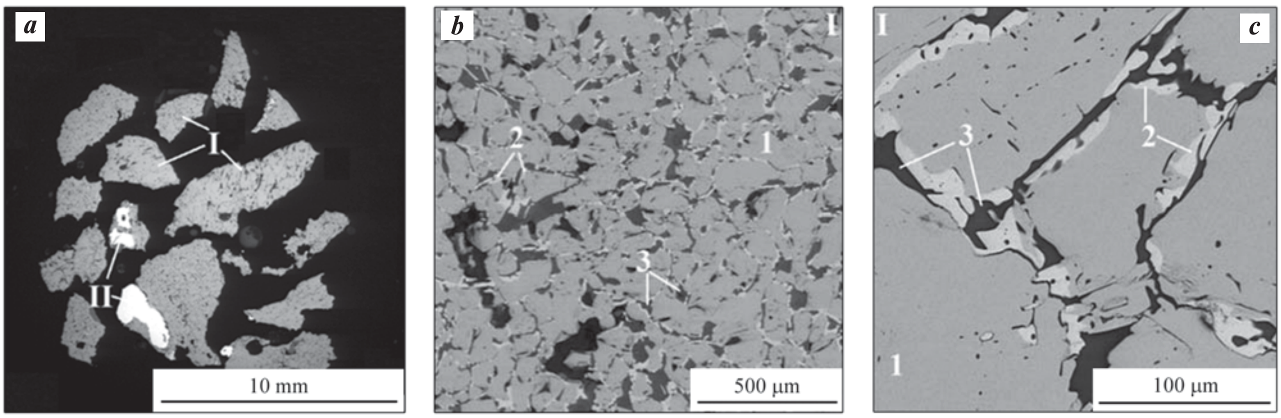

Fig. 7. General view of the oxide sample (***a***) and phase distribution (***b***, ***c***) in the analyzed material

a: I – slag particles, II – bottom phase
b, ***c***: *1* – iron oxide, *2* – copper-iron oxide, *3* – silicate phase

Рис. 7. Общий вид проб оксидной части (***a***) и распределение фаз (***b***, ***c***) в исследуемой пробе

a: I – шлаковые частицы, II – донная фаза
b, ***c***: *1* – оксид железа, *2* – оксид железа-меди, *3* – силикатная составляющая

As the data show, the magnetite-based phase formed at high temperatures cannot be removed without process adjustments or additional measures due to its high melting point. On the other hand, the high oxidation potential of the environment in which copper sulfide ores or concentrates are processed in Vanyukov furnaces does not allow the reduction of previously formed overoxidized refractory iron oxides. The primary cause of intermediate layer formation is a disruption in the operating mode of the furnace, particularly when the oxygen consumption ratio does not correspond to the composition of the processed feedstock.

To address this, thermodynamic calculations were performed to evaluate the conditions under which solid phase formation occurs in compositions close to the operational parameters of the Vanyukov furnace at the Copper Plant.

Thermodynamic modeling of copper sulfide feed oxidation

Table 2 presents the baseline compositions of the materials used in the thermodynamic calculations. These compositions are representative of the actual materials processed at the Copper Plant of PD NN. The modeling was performed using the FactSage software package [36].

The calculations were carried out in four stages. At the first stage, the process parameters were determined at t = 1300 °C obtain matte of the specified composition

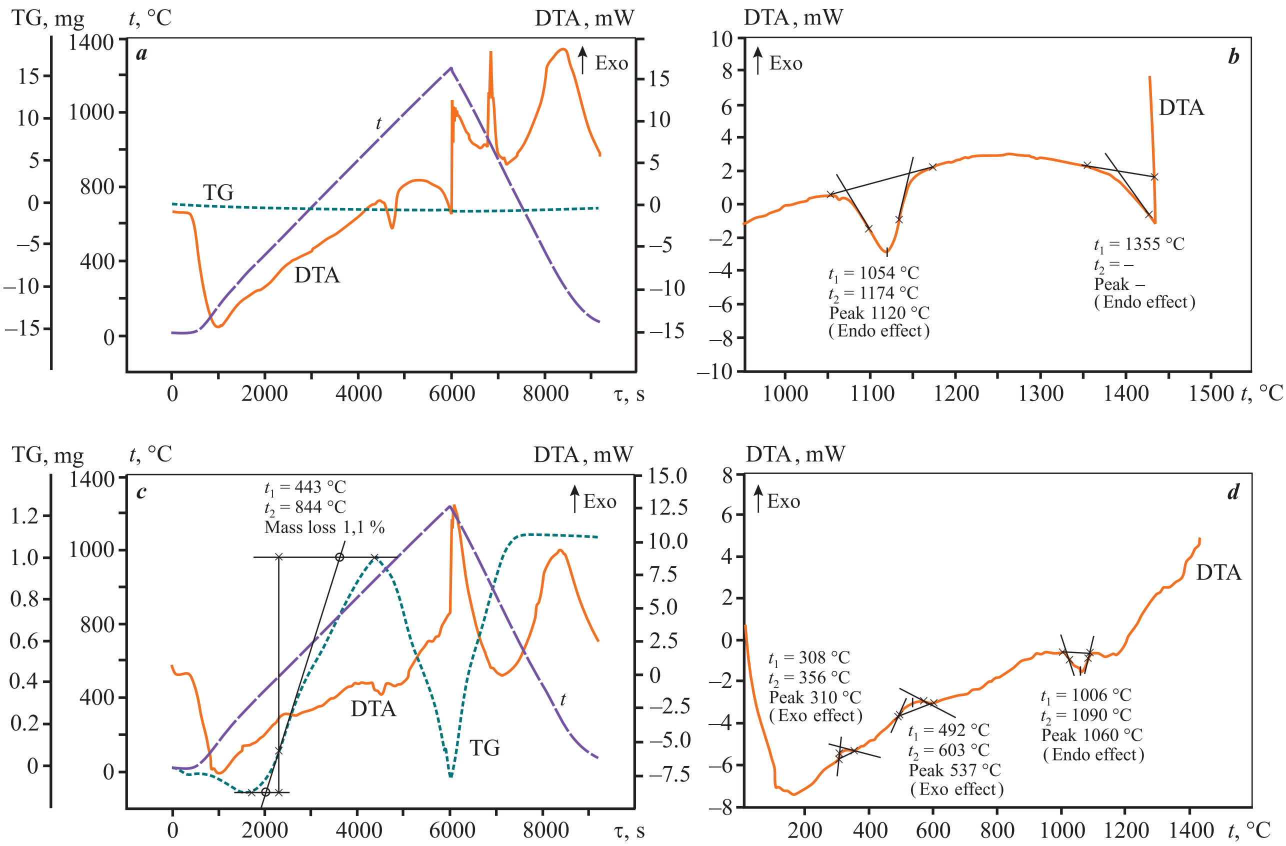

Fig. 8. TGA and DTA results for the oxide portion of the intermediate layer in argon (***a***, ***b***) and oxygen (***c***, ***d***) atmospheres

Рис. 8. Общий вид результатов ТГА и ДТА для оксидной части промежуточного слоя в атмосфере аргона (***a***, ***b***) и кислорода (***c***, ***d***)

(Fe ~15 %) and a silica content in the slag of about 30 %, which corresponds to the products obtained at the Copper Plant of the PD NN. A key requirement at this stage was the absence of solid phase formation in the system under consideration. At the second stage, the parameters established in Stage 1 were fixed, and the temperature was varied to identify the threshold conditions under which refractory compounds begin to form. At the third stage, the influence of copper concentrate—obtained from the flotation separation of nickel slag generated during copper production — on solid phase formation in the system was assessed at t = 1250 °C. The calculations were performed for a baseline case (without concentrate addition), assuming matte containing approximately 15 % Fe and slag with about 30 % SiO_2. At the fourth stage, for the slag composition from Stage 1 (where no solid phase had formed), a calculation was performed to evaluate the effect of increasing the system's oxidation potential (via oxygen addition) on solid phase formation at a fixed temperature of 1250 °C.

Thus, in Stage 1, thermodynamic modeling was performed to define conditions for the formation of a bottom phase containing ~15 wt. % Fe, with silica concentration in the slag at ~30 wt. %. The results were obtained under the following conditions: oxygen and quartzite additions of 14.8 and 17 rel. % relative to the metal-bearing feed, and a process temperature of 1300 °C.

Stages 2 to 4 were based on the parameters established at Stage 1. Solid solution phases from the software database were used in the calculations, including: Spinel-type phases of the AB_2O_4 or A_3O_4 type (with cation oxidation states 2+ and 3+); monoxides (A_xO); clinopyroxenes ($(A,B)_2SiO$); orthopyroxenes ($(Mg,Fe)_2Si_2O_6$); wollastonite ($CaSiO_3$); calcium silicate (Ca_2SiO_4); olivine ($(Mg,Fe)_2[SiO_4]$); cordierite ($Al_4Fe_2Si_5O_{18}$); mullite ($Al_6Si_2O_{13}$). Figs. 9 and 10 show the results of thermodynamic calculations, including the most stable phases within the modeled temperature range. As seen from the data, under the current calculation parameters and compositions (see Table 2), solid phase formation begins at temperatures below 1225 °C. The solid phase consists of a spinel-type magnetite phase (~25 rel. % Fe_3O_4) and clinopyroxene-group phases composed of silicates containing Fe, Mg, and Ca, with a gene-

Table 2. **Content of major components in the input feedstock materials**

Таблица 2. Содержание основных компонентов в исходных веществах

Material	Content, wt. %									
	Ni	Cu	Co	Fe	S	SiO_2	CaO	Al_2O_3	MgO	O_2
Metal-bearing feedstock	2.04	24.46	0.11	34.16	21.77	4.65	1.02	1.08	1.45	3.84
Flux	–	–	–	2.51	0.16	78	2.46	5.41	1.46	0.96
Copper concentrate (from flotation of nickel slag)	10.44	53.25	0.167	12.95	10.5	4.35	1.10	0.59	1.26	4.4
Oxidant (O_2)	–	–	–	–	–	–	–	–	–	100

ral composition of xFeSi$_2$O$_6$ (where x = Mg, Ca, Fe, Fe^{3+}). These phases account for approximately 75 rel. % of the total solid phase.

Fig. 9, *b* shows the modeling results for the effect of copper concentrate obtained from the flotation separation of copper production nickel slag on the formation of refractory phases. According to Table 2, this product is characterized by a reduced sulfur content and the presence of slag-forming components along with oxides of non-ferrous metals and iron. According to the data, at 1250 °C, the addition of more than 13 rel. % of this copper concentrate (derived from the flotation separation of nickel slag during the second stage of copper converting) to the metal-bearing charge results in the formation of refractory phases, which negatively affect the processing of the feedstock.

The study also examined slag behavior under increased oxidation potential. According to the results in Fig. 10, adding more than 1 rel. % oxygen (relative to the slag mass) disrupts equilibrium and leads to the formation of iron spinel phases similar to those identified in the experimental section. As the oxidation potential increases, the spinel fraction continues to grow, complicating the smelting process and promoting the formation of an intermediate layer rich in sulfide inclusions.

The conducted calculations indicate that deviations from standard operating conditions of the pyrometallurgical unit — whether due to changes in feed composition under a constant oxidation potential or due to increased oxidation potential with a stable feed composition — lead to the formation of high-melting compounds. These compounds cannot be decomposed under current processing conditions and, as a result, disrupt furnace operation. The destruction of such refractory phases formed at elevated temperatures inside the furnace can be achieved through chemical interaction with low-copper matte or by introducing metallized

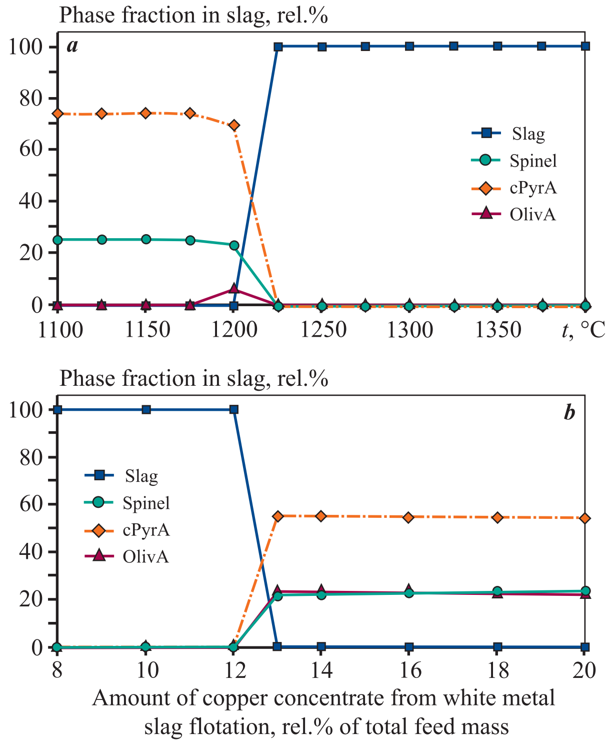

Fig. 9. Solid phase formation in slag as a function of (***a***) process temperature during oxidation of a copper-bearing sulfide charge and (***b***) the amount of copper concentrate (from white metal slag flotation) added to the charge

Spinel-type phase AB_2O_4 or A_3O_4 (oxidation states 2+ and 3+); cPyrA – clinopyroxene $(A,B)_2SiO_6$; OlivA – olivine $(Mg,Fe)_2[SiO_4]$; A and B = Fe, Fe^{3+}, Mg, Ca, Al, etc.

Рис. 9. Формирование твердой фазы в шлаке в зависимости от температуры процесса при окислении медной металлсодержащей сульфидной шихты (***a***) и от количества вводимого медного концентрата от разделения файнштейна (***b***)

Шпинель вида AB_2O_4 или A_3O_4 (степень окисления 2+ и 3+); cPyrA – клинопироксен вида $(A,B)_2SiO_6$; OlivA – оливин $(Mg,Fe)_2[SiO_4]$; A и B – Fe, Fe^{3+}, Mg, Ca, Al и др.

and carbon-containing materials. Approaches to the breakdown of high-melting compounds in flash smelting furnaces have been addressed in previous studies [37; 38].

Conclusion

The study identified the composition of the atypical product formed in Vanyukov furnaces and characterized the phase composition of the sulfide and oxide portions of the intermediate layer. The primary phase in the sulfide portion is chalcocite (Cu_2S), while the oxide portion consists of spinel, delafossite ($CuFeO_2$), cuprite (Cu_2O), and clinopyroxene with a general composition of $W_{1-p}(X,Y)_{1+p}[Z_2O_6]$, where W — Na, Ca; X — Mg, Fe^{2+}, Mn, Ni, Li; Y — Al, Fe^{3+}, Cr, Ti; Z — Si, Al.

Thermal analysis (TGA and DTA) of the sulfide phase showed a 2 rel. % mass loss in an inert atmosphere, which is attributed to the release of sulfur from non-stoichiometric Cu_2S_{1+x} as it transitions to stoichiometric Cu_2S. Endothermic effects were recorded at 1077 °C and 1100 °C, associated with the phase transformation and subsequent melting of Cu_2S (consistent with phase diagram values of 1067 °C and 1105 °C, see Fig. 5). These results indicate that the phase remains in a liquid state under Vanyukov furnace conditions and that its presence in the intermediate layer reflects mechanical entrapment within the higher-melting oxide matrix.

In an inert atmosphere, the oxide phase exhibited no change in mass. However, two endothermic effects were observed at 1057 °C (peak at 1110 °C) and 1355 °C, corresponding to the onset of melting in iron-rich oxides containing nickel and copper.

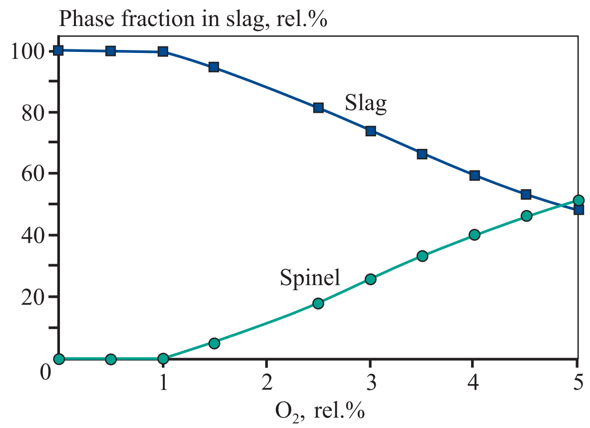

Fig. 10. Solid phase formation in slag as a function of oxidant addition to the system

Spinel-type phase AB_2O_4 or A_3O_4 (oxidation states 2+ and 3+)

Рис. 10. Формирование твердой фазы в шлаке в зависимости количества окислителя, поступающего в систему

Шпинель вида AB_2O_4 или A_3O_4 (степень окисления 2+ и 3+)

Stable operation of the Vanyukov furnace for processing the current feed composition — while avoiding the formation of refractory spinels — is constrained by the following factors:

— slag melt temperature must not fall below 1225 °c;

— the share of copper concentrate obtained from nickel slag flotation must not exceed 13 rel.% in the feed;

— excess oxidation potential in the slag system must be avoided (oxygen addition not exceeding 1 rel. %).

The results demonstrate that adjusting only the temperature of the smelting process is insufficient to eliminate the intermediate layer, since the furnace typically operates at lower temperatures (up to 1350 °C).

Thus, the most rational strategy for addressing such atypical products is to maintain strict control over the feed composition and the overall process parameters. In cases where the intermediate layer has already formed, the most effective approach to its breakdown involves chemical interaction with lean matte, the use of metallized or carbon-containing additives, and operating on lean matte to lower the oxidation potential of the system.

The findings of this study served as the basis for practical recommendations to ensure stable smelting operations in Vanyukov furnaces at the Copper Plant, particularly under conditions of fluctuating feedstock composition.

References

1. Vurdova N.G., Golubev O.V., Nedelin S.V., Petelin A.L., Polulyakh L.A., Chernousov P.I. Recycling: Textbook. Moscow: MISIS, 2020. 746 p. (In Russ.).
Вурдова Н.Г., Голубев О.В., Неделин С.В., Петелин А.Л., Полулях Л.А., Черноусов П.И. Рециклинг: Учебник. М.: МИСИС, 2020. 746 с.
2. Kandalam A, Reuter MA, Stelter M, Reinmöller M, Gräbner M, Richter A, et al. A review of top-submerged lance (TSL) processing. Part I: Plant and reactor engineering. *Metals*. 2023;13(10):1728.
http://dx.doi.org/10.3390/met13101728
3. Kandalam A, Reuter MA, Stelter M, Reinmöller M, Gräbner M, Richter A, et al. A Review of top submerged lance (TSL) processing. Part II: Thermodynamics, slag chemistry and plant flowsheets. *Metals*. 2023;13(10):1742.
http://dx.doi.org/10.3390/met13101742

4. Liu Z, Xia L. The practice of copper matte converting in China. *Mineral Processing and Extractive Metallurgy* . 2018;128(1-2):117—124.
http://dx.doi.org/10.1080/25726641.2018.1543147
5. Shibasaki T, Hayashi M. Top-blown injection smelting and converting: The Mitsubishi process. *JOM*. 1991;43(9):20—26.
http://dx.doi.org/10.1007/bf03222230
6. Swinbourne D.R., West R.C., Reed M.E., Sheeran A. Computational thermodynamic modelling of direct to blister copper smelting. *Mineral Processing and Extractive Metallurgy*. 2011;120(1):1—9.
http://dx.doi.org/10.1179/1743285510y.0000000003
7. Chen Ch., Zhang L., Jahanshahi Sh. Application of MPE model to direct-to-blister flash smelting and development of minor elements. In: *Copper International Conference: Proceeding of Copper 2013* (Santiago, Chile, 2013). P. 857—871.
https://doi.org/10.13140/2.1.4067.1360
8. Taskinen P., Kojo I. Fluxing options in the direct-to-blister copper smelting. In: *Proceedings of the VIII International Conference on Molten Slages, Fluxes and Salt — Molten 2009.* (Santiago, Chile, 2009). P. 1139—1151.
9. Sun Y.Q., Chen M., Cui Z.X., Contreras L., Zhao B.J. Phase equilibria of ferrous-calcium silicate slags in the liquid/spinel/white metal/gas system for the copper converting process. *Metallurgical and Materials Transactions: B.* 2020;5(51):2012—2020.
https://doi.org/10.1007/s11663-020-01887-9
10. Xie S., Zhao B.J. Phase equilibrium studies of nonferrous smelting slags: A review. *Metals*. 2024;14(278): 1—19.
https://doi.org/10.3390/met14030278
11. Krupnov L. V., Midyukov D. O., Malakhov P. V. Ways to cover the raw material demand in the copper-nickel sector. *Obogashchenie rud*. 2022;2:37—41. (In Russ.).
https://doi.org/10.17580/or.2022.02.06
Крупнов Л.В., Мидюков Д.О., Малахов П.В. Направления поддержания сырьевой базы медно-никелевой подотрасли. *Обогащение руд*. 2022;2:37—41.
https://doi.org/10.17580/or.2022.02.06
12. Krupnov L.V., Tsymbulov L.B., Malakhov P.V., Ozerov S.S. Operation of autogenous units in the Polar Division of Norilsk Nickel during processing of raw materials with reduced energy potential. *Tsvetnyye metally*. 2022;2:40—48. (In Russ.).
https://doi.org/10.17580/tsm.2022.02.05
Крупнов Л.В., Цымбулов Л.Б., Малахов П.В., Озеров С.С. Работа автогенных агрегатов в Заполярном филиале компании «Норникель» при переработке сырья с пониженным энергетическим потенциалом. *Цветные металлы*. 2022;2:40—48.
https://doi.org/10.17580/tsm.2022.02.05
13. Krupnov L.V., Rumyantsev D.V., Popov V.A., Malakhov P.V., Kaverzin A.V. Technical solutions to improve operating conditions of Vanyukov furnace while processing technogenic feed. *Metallurg*. 2024;4:106—111. (In Russ.). https://doi.org/10.52351/00260827_2024_4_106
Крупнов Л.В., Румянцев Д.В., Попов В.А., Малахов П.В., Каверзин А.В. Технические решения по улучшению условий эксплуатации печей Ванюкова при переработке техногенного сырья. *Металлург*. 2024;4:106—111.
https://doi.org/10.52351/00260827_2024_4_106
14. Taskinen P, Jokilaakso A. reaction sequences in flash smelting and converting furnaces: An in-depth view. *Metallurgical and Materials Transactions: B.* 2021; 52(5):3524—3542.
http://dx.doi.org/10.1007/s11663-021-02283-7
15. Krupnov L.V. Mechanism of refractory accretion formation in flash smelting furnaces and methods of accretion removal: Abstract of the dissertation of Cand. Sci. (Eng.). St. Petersburg: Federal State Budgetary Educational Institution of Higher Education “Saint Petersburg Mining University”, 2015. 19 p. (In Russ.).
Крупнов Л.В. Механизм образования тугоплавкой настыли в печах взвешенной плавки и способы ее устранения: Автореф. дис. ... канд. техн. наук. СПб, Национальный минерально-сырьевой ун-т «Горный», 2015. 19 с.
16. Kaur R., Nexhip C., Krippner D., George-Kennedy D., Routledge M. “Double Flash” technology after 16 years. In: *Papers to be presented at the thirteenth International Flash Smelting Congress* (2—8 October 2011, Zambia). Livingstone, Africa, 2011. 13 p.
17. Jiménez F., Ramos M., Pérez I. A review of recent improvements to control weak acid production at the Huelva smelter. In: *Papers to be presented at the thirteenth International Flash Smelting Congress* (2—8 October 2011, Zambia). Livingstone, Africa, 2011. 22 p.
18. Crundwell F.K., Moats M.S., Ramachandran V., Robinson T.G., Davenport W.G. Flash smelting of nickel sulfide concentrates. *Extractive Metallurgy of Nickel, Cobalt and Platinum Group Metals*. 2011;215—232.
http://dx.doi.org/10.1016/b978-0-08-096809-4.10018-8
19. Zhao B., Hayes P., Jak E. Effects of CaO, Al_2O_3 and MgO on liquidus temperatures of copper smelting and converting slags under controlled oxygen partial pressures. *Journal of Mining and Metallurgy, Section B: Metallurgy.* 2013;49(2):153—159.
http://dx.doi.org/10.2298/jmmb120812009z
20. Xie S., Yuan X., Liu F., Zhao B. Control of copper content in flash smelting slag and the recovery of valuable metals from slag. *A Thermodynamic Consideration Metals.* 2023;13(1):153. http://dx.doi.org/10.3390/met13010153

21. Kojo I., Storch H. Copper production with Outokumpu flash smelting: an update. In: *International Symposium on Sulfide smelting 2006. Vol. 8: Sohn International Symposium. Advanced Processing of Metals and Materials. The Minerals, Metals & Materials Society*. San Diego, California, USA, 2006. P.225—238.
22. Wang G., Cui Y., Li X., Shi R., Yang J., Yang S. et al. Structure and adaptability of $Fe_xO—SiO_2—MgO—$15 wt. % CaO—0.026 wt. % NiO slag with the Fe/SiO_2 mass ratio of 1.2 in flash matte smelting. *Ceramics International*. 2023;49(2):2531—2539.
http://dx.doi.org/10.1016/j.ceramint.2022.09.232
23. Yakimov I.S. System of *X*-ray phase identification of essentially multiphase materials. *Zavodskaya laboratoriya. Diagnostika materialov*. 2007;11(73):32—37. (In Russ.).
Якимов И.С. Система рентгенофазовой идентификации существенно многофазных материалов. *Заводская лаборатория. Диагностика материалов*. 2007;11(73):32—37.
24. Yakimov I.S., Dubinin P.S., Piksina O.E. Regularized multireflex method of reference intensities for quantitative *X*-ray phase analysis of polycrystalline materials. *Zavodskaya laboratoriya. Diagnostika materialov*. 2009;12(76):71—80. (In Russ.).
Якимов И.С., Дубинин П.С., Пиксина О.Е. Регуляризированный мультирефлексный метод ссылочных интенсивностей для количественного рентгенофазового анализа поликристаллических материалов. *Заводская лаборатория. Диагностика материалов*. 2009;12(76):71—80.
25. Piksina O.E., Ruzhnikov S.G., Dubinin P.S. *X*-ray spectral analysis: guidelines — Materials science and technology of new materials. Krasnoyarsk: SibFU, 2012. 43 p. (In Russ.).
Пиксина О.Е., Ружников С.Г., Дубинин П.С. Рентгеновский спектральный анализ: Методические указания. Материаловедение и технология новых материалов. Красноярск: СибФУ, 2012. 43 с.
26. Kolesnikov A.S. Kinetic investigations into the distillation of nonferrous metals during complex processing of waste of metallurgical industry. *Russian Journal of Non-Ferrous Metals*. 2015;56(1):1—5.
https://doi.org/10.3103/S1067821215010113
27. Kolesnikov A.S., Serikbaev B.E., Kenzhibaeva G.S., Botabaev N.E., Shapalov S.K., Kolesnikova O.G., Iztleuov G.M., Suigenbayeva A.A., Asylbekova D.D., Ashirbaev K.A., Kolesnikova V.A., Zolkin A.L., Isaev G.I., Alchinbaeva O.Z., Kutzhanova A.N. Processing of non-ferrous metallurgy waste slag for its complex recovery as a secondary mineral raw material. *Refractories and Industrial Ceramics*. 2021;62(4):375—380.
https://doi.org/10.1007/s11148-021-00611-7
28. Kolesnikov A.S., Kenzhibaeva G.S., Botabaev N.E., Kutzhanova A.N., Iztleuov G.M., Suigenbaeva A.Z., Ashirbaev K.A., Kolesnikova O.G. Thermodynamic modeling of chemical and phase transformations in a waelz process-slag — carbon system. *Refractories and Industrial Ceramics*. 2021;61(3):289—292.
https://doi.org/10.1007/s11148-020-00474-4
29. Kolesnikov A., Fediuk R., Amran M., Klyuev S., Klyuev A., Volokitina I., Naukenova A., Shapalov S., Utelbayeva A., Kolesnikova O., Bazarkhankyzy A. Modeling of non-ferrous metallurgy waste disposal with the production of iron silicides and zinc distillation. *Materials*. 2022;15(7):1—14.
https://doi.org/10.3390/ma15072542
30. Zhanikulov N., Kolesnikov A.S., Taimasov B.T., Zhakipbayev B.Y., Shal A.L. Influence of industrial waste on the structure of environmentally friendly cement clinker. *Complex Use of Mineral Resources*. 2022;4(323):84—91.
https://doi.org/10.31643/2022/6445.44
31. Kolesnikov A.S. Thermodynamic simulation of silicon and iron reduction and zinc and lead distillation in zincoligonite ore-carbon systems. *Russian Journal of Non-Ferrous Metals*. 2014;55(6):513—518.
https://doi.org/10.3103/S1067821214060121
32. Donayev A., Kolesnikov A., Shapalov Sh., Sapargaliyeva B., Ivakhniyuk G. Studies of waste from the mining and metallurgical industry, with the determination of its impact on the life of the population. *News of the National Academy of Sciences of the Republic of Kazakhstan. Series of Geology and Technical Sciences*. 2022;4(454):55—68.
https://doi.org/10.32014/2022.2518-170x.200
33. Sharma R.C., Chang Y.A. A thermodynamic analysis of the copper-sulfur system. *Metall Transactions: B*. 1980;11:575—583. https://doi.org/10.1007/BF02670137
34. Bannykh O.A., Budberg P.B., Alisova S.P., Drits M.E. State diagrams of binary and multicomponent systems based on iron: Handbook. Moscow: Metallurgiya, 1986. 440 p. (In Russ.).
Банных О.А., Будберг П.Б., Алисова С.П., Дриц М.Е. Диаграммы состояния двойных и многокомпонентных систем на основе железа: Справочник. М.: Металлургия, 1986. 440 с.
35. Levin M., Robbins C.R., McMurdie H.F. Phase diagrams for ceramists. The American Ceramic Society. Columbus, Ohio. 1964. 601 p.
36. Bale C. W., Bélisle E., Chartrand P., Decterov S. A., Eriksson G., Gheribi A.E., Hack K., Jung I.H., Kang Y.B., Melançon J., Pelton A.D., Petersen S., Robelin C.. Sangster J., Spencer P., Van Ende M-A. FactSage thermochemical software and databases 2010—2016. *Calphad*. 2016;54:35—53.
https://doi.org/10.1016/j.calphad.2016.05.002
37. Krupnov L.V., Starykh R.V., Petrov A.F. Mechanism of

formation of refractory crust in flash smelting furnaces of Nadezhda metallurgical plant. *Tsvetnye metally*. 2013;(2):46—49. (In Russ.).

Крупнов Л.В., Старых Р.В., Петров А.Ф. Механизм формирования тугоплавкой настыли в печах взвешенной плавки Надеждинского металлургического завода. *Цветные металлы*. 2013;(2):46—49.

38. Krupnov L.V., Pakhomov R.A., Kaverzin A.V., Kosov Ya.I., Malakhov P.V. Study of properties of intermediate layer formed in Vanyukov furnace while processing nickel-containing copper feed. In: Books of reports of the 12th International Congress of Non-Ferrous Metals and Minerals – 2024. Krasnoyarsk: 2024. P. 897—899. (In Russ.).

Крупнов Л.В., Пахомов Р.А., Каверзин А.В., Косов Я.И., Малахов П.М. Изучение свойств промежуточного слоя печей Ванюкова при переработке медного никельсодержащего сырья. В сб.: *Сборник докладов 12-го международного конгресса Цветные Металлы и Минералы — 2024.* (Красноярск, 09—13 сентября 2024 г.). Красноярск: Научно-инновационный центр, 2024. С. 883—888.

Information about the authors

Leonid V. Krupnov – Cand. Sci. (Eng), Chief Metallurgist, Head for Process Planning and Monitoring at the Science and Technology Department, Polar Division of PJSC «MMC «Norilsk Nickel»; Associate Professor at the Department of Non-Ferrous Metallurgy, N.M. Fedorovsky Polar State University.
https://orcid.org/0009-0008-7451-9610
E-mail: KrupnovLV@nornik.ru

Roman A. Pakhomov – Cand. Sci. (Eng), Senior Researcherof the Department of Research and Development of the Pyrometallurgy laboratory, LLC Gipronikel Institute.
https://orcid.org/0000-0002-9099-8059
E-mail: Pakhomovra@gmail.com

Anton V. Kaverzin – Senior Lecturer, Department of Non-Ferrous Metallurgy, N.M. Fedorovsky Polar State University.
https://orcid.org/0009-0001-4985-0044
E-mail: KaverzinAV@norvuz.ru

Yaroslav I. Kosov – Cand. Sci. (Eng), Researcher, Department of Research and Development of the Pyrometallurgy laboratory, LLC Gipronikel Institute.
https://orcid.org/0000-0001-7993-2799
E-mail: KosovYaI@nornik.ru

Pavel V. Malakhov – Main Engineer, Center for Engineering Support of Production, Polar Division of PJSC «MMC «Norilsk Nickel».
https://orcid.org/0009-0006-7189-5616
E-mail: MalakhovPV@nornik.ru

Информация об авторах

Леонид Владимирович Крупнов – к.т.н., гл. металлург, начальник управления технологического планирования и контроля научно-технического департамента, Заполярный филиал ПАО «ГМК «Норильский никель»; доцент кафедры металлургии цветных металлов, Заполярный государственный университет им. Н.М. Федоровского.
https://orcid.org/0009-0008-7451-9610
E-mail: KrupnovLV@nornik.ru

Роман Александрович Пахомов – к.т.н., ст. науч. сотрудник департамента по исследованиям и разработкам лаборатории пирометаллургии, ООО «Институт Гипроникель».
https://orcid.org/0000-0002-9099-8059
E-mail: Pakhomovra@gmail.com

Антон Викторович Каверзин – ст. преподаватель кафедры металлургии цветных металлов, Заполярный государственный университет им. Н.М. Федоровского.
https://orcid.org/0009-0001-4985-0044
E-mail: KaverzinAV@norvuz.ru

Ярослав Игоревич Косов – к.т.н., науч. сотрудник департамента по исследованиям и разработкам лаборатории пирометаллургии, ООО «Институт Гипроникель.
https://orcid.org/0000-0001-7993-2799
E-mail: KosovYaI@nornik.ru

Павел Вячеславович Малахов – гл. инженер Центра инженерного сопровождения производства, Заполярный филиал ПАО «ГМК «Норильский никель».
https://orcid.org/0009-0006-7189-5616
E-mail: MalakhovPV@nornik.ru

Contribution of the authors

L.V. Krupnov – development of the main concept, scientific supervision, formulation of the research goals and objectives, preparation of the manuscript, formulation of conclusions.

R.A. Pakhomov – thermodynamic modeling, supervision of experimental studies (TGA, DTA, SEM, EPMA, etc.), contribution to manuscript preparation.

A.V. Kaverzin – experiment setup and execution, thermodynamic calculations, analysis of experimental results.

Ya.I. Kosov – text editing and formatting, analysis of research results, refinement of conclusions.

P.V. Malakhov – resource support, planning and execution of experiments, contribution to the conceptual framework, formulation of research goals and objectives, manuscript writing, and conclusion development.

Вклад авторов

Л.В. Крупнов – формирование основной концепции, научное руководство, постановка цели и задачи исследования, подготовка текста, формулировка выводов.

Р.А. Пахомов – осуществление расчетов, курирование проведения экспериментальных исследований (ТГА и ДТА, РЭМ и РСМА и др.), подготовка текста статьи.

А.В. Каверзин – подготовка и проведение экспериментов, выполнение расчетов, анализ результатов исследований.

Я.И. Косов – корректировка и оформление текста, анализ результатов исследований, корректировка выводов.

П.В. Малахов – обеспечение ресурсами, подготовка и проведение экспериментов, формирование основной концепции, постановка цели и задачи исследования, подготовка текста, формулировка выводов.

The article was submitted 23.08.2024, revised 20.11.2024, accepted for publication 25.11.2024

Статья поступила в редакцию 23.08.2024, доработана 20.11.2024, подписана в печать 25.11.2024